Al-Qadisiyah JournalFor Engineering Sciences 18 (2025) 148 – 154

Contents lists available at: http://qu.edu.iq

Al-Qadisiyah Journal for Engineering Sciences

Journal homepage: https://qjes.qu.edu.iq

Research Paper

Surrogated based optimization of stress concentration in Al-2024 T3 plate with elliptical cutout under uniaxial loading

Rwaa Talal Abdullah [1]✉, ***Omar D. Jumaah*** [1], ***and Yogesh Jaluria*** [2]

[1]*Mechanical Engineering Department, College of Engineering, University of Mosul, 41002, Mosul, Iraq.*
[2]*Department of Mechanical and Aerospace Engineering, Rutgers, The State University of New Jersey, 08854, NJ, USA.*

ARTICLE INFO

Article history:
Received 23 August 2024
Received in revised form 29 December 2024
Accepted 24 May 2025

keyword:
Stress concentration factor
Elliptical cutout
Cutout orientation angle
Auxiliary holes
Multi-objective optimization
Response surface model
Pareto frontier

ABSTRACT

Metal plates with different cutout shapes are commonly used in various engineering applications. Cutouts are unavoidable in structural design as they are needed for practical reasons, such as reducing the structure's weight and providing access to other parts. This paper investigates the stress concentration induced in Al-2024 T3 plate with an elliptical cutout under a tensile load, experimentally and numerically. Practical tensile test and strain gauge results measure the generated stress concentration in Al-2024 T3 plate. A finite element model is created to analyze the stress concentration factor (SCF) in Al 2024 T3 plate under uniaxial loading. The numerical model is validated against the experimental and analytical results. The influence of the elliptical cutout orientation angle (ϕ) on SCF was investigated. The results showed that SCF increases with increasing elliptical cutout orientation angle (ϕ = 0°) to (ϕ= 90°). However, adding auxiliary holes around the central elliptical cutout enhances the stress distribution and reduces SCF in the range (1.9 to 25%). Surrogated-based optimization is used to build response surface models for predicting optimal SCF and removal mass (RM). Multi-objective optimization is formulated to minimize SCF and maximize RM. The results show that increasing AH diameter leads to minimizing SCF and maximizing RM for the plate with an elliptical cutout that is restrained to be greater than or equal to 45 ($\phi \geq 45°$). Pareto frontier offers reliable, optimal solutions of SCF and RM based on input design parameters, including the orientation angle and auxiliary hole diameters.

1. Introduction

In recent years, structural shape optimization has attracted attention to justify the increasing need for lightweight and efficient systems [1]. Metal plates with cutouts are commonly used in aerospace, automotive structures, and various engineering applications [2]. Different cutout shapes in structural elements are needed for practical reasons, such as design requirements, reducing the structure's weight, and providing access to other parts [3]. For example, window and door openings in aircraft fuselages require elliptic configuration cutouts [4]. However, the presence of these cutouts induces stress concentration, which is a critical factor in mechanical parts failure [5]. Thus, minimizing the stress concentration around cutouts is essential [6]. Different methods are proposed to determine plate stress concentration factors (SCF) [7]. Graphical forms and charts were proposed based on mathematical analysis for evaluating stress concentration factors in isotropic plates with discontinuities [8]. Bharambe and Kolhe [9] used finite element analysis (FEA), analytical approach, and experimental analysis to perform the stress concentration in mild steel plates with rectangular cutouts. The results show that the loading direction significantly influences the stress concentration. Rezaeepazhand and Jafari [10] conducted an analytical investigation to analyze the stress distribution in perforated plates with central holes. The results revealed that SFC can be altered by adjusting cutout parameters, including shape, size, bluntness, and orientation. Kumar et al. [11] analyzed the stress concentration of perforated aluminum plates that have polygonal cutouts with different shapes and bluntness. The results showed that the stress concentration increased when cutouts became perpendicular to the applied load direction. Patil and More [12] studied the effect of hexagonal cutout roundness and orientation on stress concentration in a plate under tensile loading. Aligning the hexagonal cutout's vertical axis of symmetry parallel to the applied tensile load reduces stress concentration. Jafari and Ardalani [13] used a complex variable technique based on the conformal mapping function to study the stress distribution around different regular holes in finite isotropic plates under the uniaxial loading. The results showed that using the theory of infinite plates to study stress distribution in finite plates could lead to significant errors. Lu et al. [14] investigated minimizing the stress concentration around an elliptical hole in a uniaxially loaded plate by applying concentrated forces. The optimization method, complex potential, was used to minimize the tangential stress concentration and determine the optimum positions and values of the concentration forces. Optimizing the applied concentrated forces can significantly decrease the tangential stress field around the hole. The results showed that the final SCF can be reduced by nearly 38% compared with the initial value. Monti [15] proposed the C-shaped void pattern to reduce the local stress field around a circular hole. Airy's stress function and ABAQUS software were used to examine the distribution of the local Endigeri and Sarganachari [16] analyzed SCF in the composite plate using a numerical model based on finite element method (FEM) (ANSYS 9.0). The model is used to predict the optimum location and optimum radii of auxiliary holes (AH). It is observed that the presence of AH reduced the stress concentration factor by (9 to 28 %) compared with initial values. The location and value of maximum stress are affected by many parameters, such as cutout size, shape, location, and orientation.

*Corresponding Author.
E-mail address: rwaa.abdallah@uomosul.edu.iq ; Tel: (+964 770-208 4989) (Rwaa Abdullah)

https://doi.org/10.30772/qjes.2024.153041.1371

Nomenclature

AH	Auxiliary Holes
APDL	ANSYS Parametric Design Language
CD	Central Distance (*mm*)
DOE	Design of Experiments
E	Young modulus (*GPa*)
FEM	Finite Element Method
RM	Removal Mass
RSM	Response Surface Method
SCF	Stress Concentration Factor
Z	A variable represents SCF or RM in the quadratic model
Greek Symbols	
ϕ	orientation angle (Degree)
ν	Poisson ratio
σ_{max}	Maximum-stress value (*MPa*)
c	Coefficients of the quadratic model
σ	stress (*MPa*)
ε	Strain
Subscripts	
d	Auxiliary holes diameter (*mm*)
deg.	Degree
Min	Minimize the objective function
Max	Maximize the objective function

Rani et al. [17] employed the extended finite element method and Matlab code to investigate stress concentration in a finite panel with a central elliptical inclusion coated by functionally graded material (FGM) subjected to uniaxial tension. The results show that a higher coating can significantly lower the stress concentration. It is revealed from the literature that many researchers investigated stress concentration in a finite plate with various cutouts using experimental, analytical, and numerical analysis. However, the effect of the elliptical cutout on stress distribution still attracts attention. Thus, applying optimization techniques to identify the best possible design parameters to reduce the stress concentration in plates with cutouts is desirable.

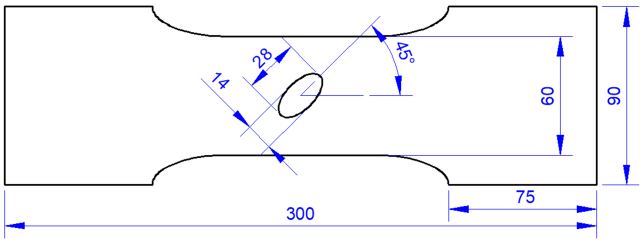

Figure 1. Experimental specimen dimensions (mm) of Al-2024 T3 plate with oriented elliptical cutout.

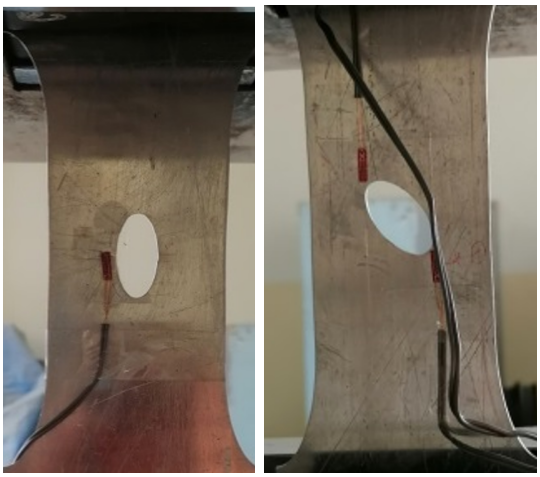

(a) $\phi = 0°$ (b) $\phi = 45°$

Figure 2. Tensile test specimen of Al-2024 T3 plate with oriented elliptical cutout. Strain gauges are fixed near cutout edges at specified positions.

This paper investigates the effect of elliptical cutout orientation angle on the stress concentration in Al-2024 T3 alloy plates under tensile load, experimentally and numerically. Also, it uses surrogate-based optimization to predict the optimal process parameters to minimize the SCF in Al-2024 T3 alloy plates with elliptical cutouts under tensile loading. Surrogate-based optimization is an efficient technique for finding the optimal solution for structure design [18]. It is an effective method in reducing the time and cost consumed to find optimum design parameters. The objective of the surrogate model is to construct an approximate mathematical model based on sampled points to predict the relationship between inputs and outputs of the process [19]. The design of experiments (DOE) determines multiple combinations of the controlled sample points that provide adequate coverage of the design space without variation [20]. Various techniques have been developed to achieve the exact best fit with single or multiple variables. The response surface method (RSM) typically efficiently compromises the modeling precision and computational expense [21]. It can reduce numerical noise in data and effectively capture the global trend of the variation [22]. Thus, RSM is robust and well-suited for addressing optimization design parameters. The most common surrogate model for creating a response surface is a polynomial response surface [23].

2. Experimental setup

A modified shape specimen is adopted from [24] to study the stress concentration in the plate. The model is used to ensure that failure occurs in the middle of the specimen. The Al-2024 T3 alloy plate specimen has a length of $L = 300$ *mm*, a gauge width $W = 60$ *mm*, and a thickness of $t = 1.2$ *mm*, with an elliptical central cutout $2a = 28$ *mm* and $2b = 14$ *mm*, as shown in Fig. 1. Specimens are cut from the Al-2024 sheet along a rolling direction using a CNC milling machine with high accuracy. The model material properties are Poisson ratio $\nu = 0.33$, Young modulus $E = 71$ *GPa*. Tensile tests were done on a universal testing machine of a capacity (100 Tons) in the material testing laboratory at Civil Engineering Department, as shown in Fig. 2. For the analysis, the applied load was controlled intentionally to limit the resulting stress in the elastic range and far below the yield point. Thus, the model is subjected to a uniform loading force ($P = 9.8$ *KN*) with the same constant strain rate for all specimens. The strain gauge is bonded at the top surface of the plate near the edge of the elliptical cutout. A linear strain gauge (Tokyo measuring instrument, Lab.) with a length of 5 *mm*, a resistance of 118.5 ± 0.5 *Ohms*, and a gauge factor of $2.10 \pm 1\%$ was used to measure the strain. Strain gauges are located at position coordinates measured from the center of the specimen ($X = 0$, $Y = 0$). The position coordinates of elliptical cutouts with $\phi = 0°$and $\phi = 45°$, are ($X = -12$, $Y = 0$), and ($X = -12, -12$ and $Y = 15, -15$), respectvely.

3. Numerical analysis

A code of multiple commands was constructed to generate a numerical model based on the given geometry dimensions and mechanical properties of Al-2024 T3 plate. ANSYS Parametric Design Language (APDL) 2022R1 simulates the model [25]. This study selected a solid Plane183 element to generate the mesh. A fine mesh was set near the cutout edges to capture the stress variation effectively, and a sufficient mesh was set elsewhere in the model, as shown in Fig. 3. The mesh number equals 7636, and the nodes equals 23760. An independent mesh study was conducted to achieve accurate results for the SCF. A uniform tensile load ($P = 9.8$ *KN*) is applied on the right side, and the left side is fixed to ensure a static equilibrium. The maximum stress σ_{max} is measured at the edge of the elliptical cutout. The normal stress σ_{nom} equals the average stress along a path plotted across the width of the gauge length. The numerical simulation for stress distribution of Al-2024 T3 plate with elliptical cutouts is shown in Fig. 4. Since the local stress is proportional to the strain ($\sigma = \varepsilon E$), the experimental stress value at the same location of the strain gauge can be obtained as shown in Table 1. The experimental and numerical model results show good agreement, which resulted in an error of less than 6.15 %. The gross stress concentration factor K_{tg} of finite-width plate with a central elliptical cutout can be determined analytically, Eq. 1 up to Eq. 5, [26].

$$SCF = K_{tg} = \frac{\sigma_{max}}{\sigma_{nom}} = \frac{\sigma_{max}}{P} Wt \tag{1}$$

$$K_{tn} = \frac{\sigma_{max}}{P} Wt \left(1 - \frac{2a}{W}\right) = K_{tg} \left(1 - \frac{2a}{W}\right) \tag{2}$$

$$K_{tg} = K_{tn}\left(1-\frac{2a}{W}\right)^{-1} \tag{3}$$

$$K_{tn} = C_1 + C_2\left(\frac{2a}{W}\right) + C_3\left(\frac{2a}{W}\right)^2 + C_4\left(\frac{2a}{W}\right)^3 \tag{4}$$

$$\begin{aligned} C_1 &= +1.000 + 0.000 \times \sqrt{a/b} + 2.000 \times (a/b) \\ C_2 &= -0.351 - 0.021 \times \sqrt{a/b} - 2.483 \times (a/b) \\ C_3 &= +3.621 - 5.183 \times \sqrt{a/b} + 4.490 \times (a/b) \\ C_4 &= -2.270 + 5.204 \times \sqrt{a/b} - 4.011 \times (a/b) \end{aligned} \tag{5}$$

Table 1. Comparison between experimental and numerical results of the local strain and stress, respectively.

ϕ	Experimental		Numerical		Error%
	$\varepsilon \times 10^{-3}$	$\sigma(MPa)$	$\varepsilon \times 10^{-3}$	$\sigma(MPa)$	
0°	3.14	229.07	3.14	232.74	1.6
45°	2.675	189.92	2.85	202.35	6.15
90°	7.03	499.46	7.11	513.6	2.64

Table 2. Comparison between analytical and numerical model results.

ϕ	(a/b)	Analytical		Numerical model			Error%
		K_{tn}	K_{tg}	σ_{nom}	σ_{max}	SCF	
0°	2/1	1.737	2.266	138.78	304	2.21	2.08
90°	1/2	3.356	6.293	138.78	886	6.51	3.02

Where σ_{max} is maximum stress at the cutout, σ_{nom} is normal stress, P is applied load, W is width at the gauge length zone, t is the thickness, and K_{tn} is the net stress concentration factor. Table 2 reveals a good match between the analytical and numerical model results, resulting in an error of less than 3.02 %. As a result, the model is valid and reliable for simulated stress concentration in Al 2024 T3.

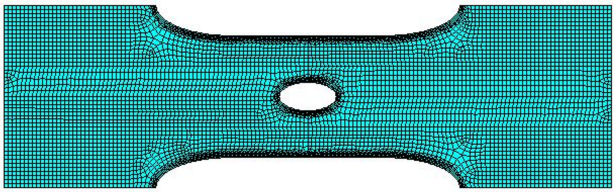

Figure 3. Meshing of the numerical model with an elliptical cutout (ϕ = 0°).

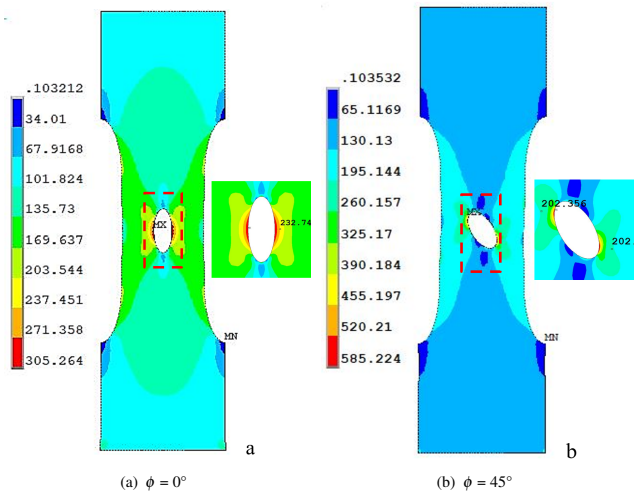

Figure 4. Tensile test specimen of Al-2024 T3 plate with oriented elliptical cutout. Strain gauges are fixed near cutout edges at specified positions.

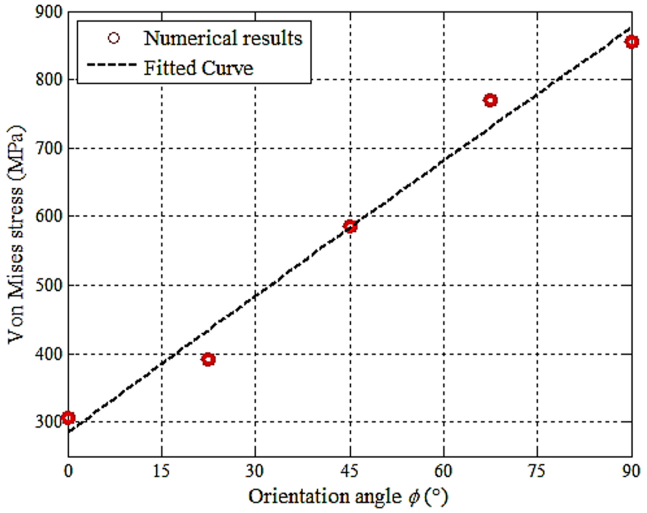

Figure 5. The corresponding Von Mises stress versus the orientation angle of the elliptical cutout in Al-2024 T3 plate.

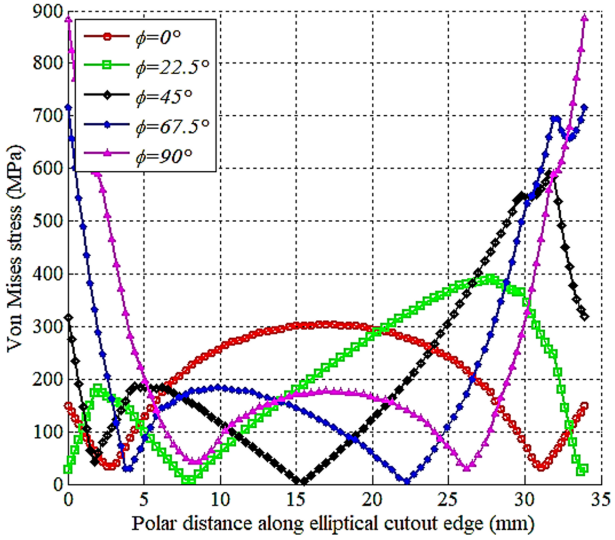

Figure 6. Stress distribution along edges of the central elliptical cutout in Al-2024 T3 plate at different orientation angles.

3.1 The orientation angle (ϕ)

The influence of the elliptical cutout orientation angle on stress concentration was investigated. Under the same loading condition, Von Mises stress and SCF varied due to the changing cutout orientation angle. Figure 5 demonstrates the variation of Von Mises stress with respect to the orientation angle of the elliptical cutout. It is observed that the maximum stress increases with increasing the orientation angle from ($\phi = 0°$) to ($\phi = 90°$). The maximum value of Von Mises stress occurred at an orientation angle of ($\phi = 90°$), resulting in higher stress concentration. High values of Von Mises stress occurred on both sides of the cutout when it was aligned perpendicular to the uniaxial tensile loading direction. That means a lower value of Von Mises stress occurred when the cutout aligned horizontally ($\phi = 0°$) with the applied loading compared with other orientation angles. Figure 6 shows the stress distribution around the edges of the elliptical cutout for five orientation angles. It is observed that the elliptical cutout oriented by ($\phi = 90°$) has a higher stress at the cutout edges compared with other orientation angles. The existence of elliptical cutouts will lead to a high-stress concentration at cutout edges that may be subjected to local yielding. The analysis shows that the residual stress will be redistributed to the adjacent areas of the plate cross-section after the plate reaches the yield zone [24]. Thus, due to its ductile nature, Al-2024 T3 plate can deform without fracture under normal conditions. Moreover, to prevent a fracture in the net

section of the plate, the applied stress should be less than the ultimate tensile strength of the used material. The results show that a plate with an elliptical cutout that is oriented by an angle of more than $\phi = 45°$has a higher stress concentration. Thus, critical case studies are selected based on the maximum stress values to predict the optimal design that enhances the stress distribution and reduces the SCF.

4. Mitigation of SCF

In mechanical engineering design, it is important to minimize the stress concentration to avoid failure in parts. Many methods have been proposed in the literature for reducing SCF around any discontinuity [27]. The literature has previously noted that SCF can be mitigated by adding auxiliary holes (AH) [28]. The AH hole radii and the central distance between the main cutout and the AH hole can affect the stress concentration factor [29]. However, selecting an appropriate size and location for these holes is still up to trial and error or may be achieved through exploration. We considered introducing circular auxiliary holes (AH) with varying diameters, d, to enhance the stress distribution and mitigate the SCF in the Al-2024 T3 plate.

4.1 Auxiliary hole size

Al-2024 T3 plate has an elliptical cutout, and AH with different diameters (6 to 24 *mm*) is analyzed. Figure 7 shows the stress flow in the Al-2024 T3 plate with AH, one on each side of the central elliptical cutout. The presence of auxiliary holes can reduce the total cross-sectional area. Also, it is observed that AH modifies the stress distribution shape around the central cutout, which reduces the maximum stress value.

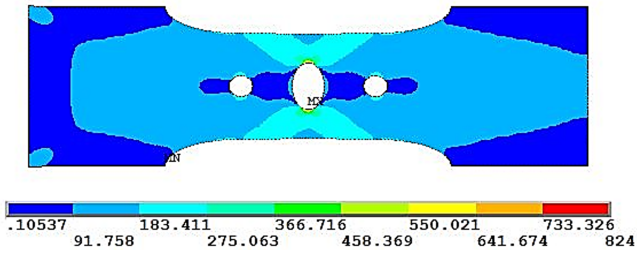

Figure 7. The stress distribution of Al-2024 T3 plate with elliptical cutout ($\phi = 90°$) and auxiliary holes ($d = 12$ *mm*).

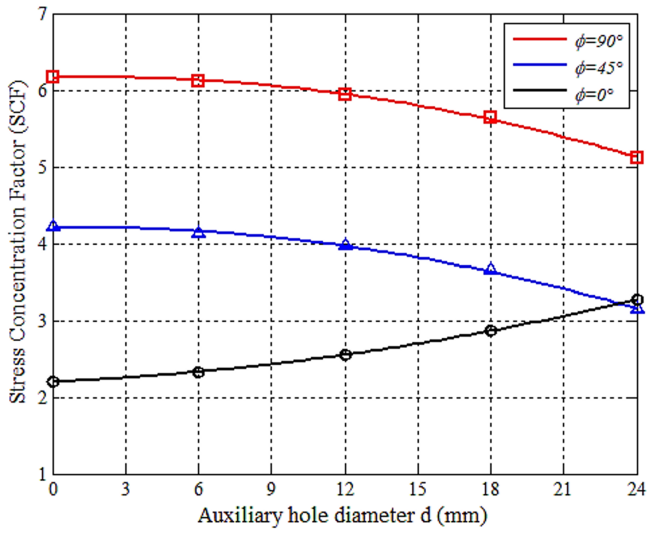

Figure 8. Effect of AH diameter on SCF in Al-2024 T3 plate with different oriented elliptical cutouts.

Figure 8 shows the stress concentration factor (SCF) plotted as a function of AH diameter for a plate with an elliptical cutout oriented by different angles. In Fig. 8, when $d = 0$, means no AH is added to the plate. The presence of AH with different diameters (d = 6 to 24 *mm*) near the elliptical cutout alters the flow stress in the plate. It is worth mentioning that adding AH for a plate with an elliptical cutout aligned horizontally ($\phi = 0°$) increases the maximum stress gradually with increasing AH diameter, as shown in Fig. 9. A similar behavior is confirmed by Yang [29], as the maximum stress of the plate under loading is located at the edges of larger holes due to the complicated interaction between auxiliary holes and the central cutout. In contrast, the maximum stress in the plate with an oriented elliptical cutout by angle ($\phi \geq 22.5°$) decreases when adding AH. As a result, adding AH reduces the maximum stress value (σ_{max}) and decreases SCF. Adding *AH* means more material is removed from the plate, reducing the plate's total mass. Table 3 shows the amount of removed mass from the plate with the central cutout and auxiliary holes for different diameters. It is worth noting that the presence of auxiliary holes helps reduce the overall mass of the plate and thereby effectively enhances the strength-weight ratio, which is essential for the automotive and aviation industries.

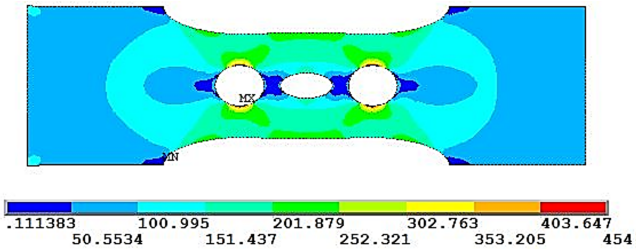

Figure 9. The stress distribution of Al-2024 T3 plate with elliptical cutout ($\phi = 0°$) and auxiliary holes ($d = 24$ *mm*).

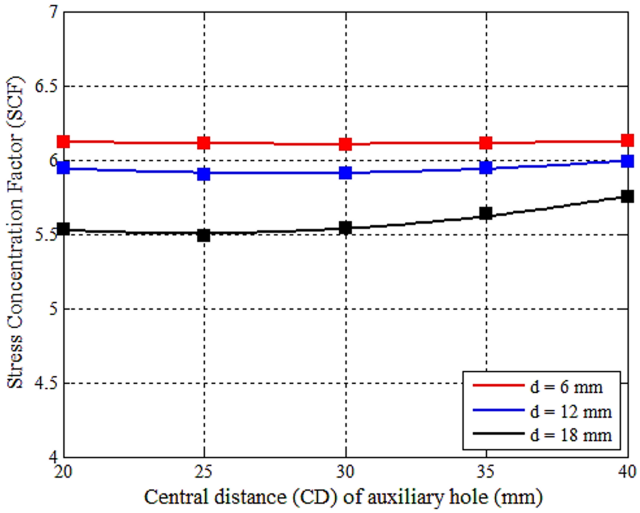

Figure 10. Effect of the central distance of AH on SCF in Al-2024 T3 plate with elliptical cutout ($\phi = 90°$) for different AH diameters.

Table 3. Mass reduction due to auxiliary holes.

Plate's total mass (g)	67.49	—	—	—
AH diameter, d (mm)	06.00	12.00	18.00	24.00
Removed mass, RM (g)	0.1800	00.74	01.65	02.94
Percentage % of removed mass	0.2667	1.0965	2.445	4.356

4.2 The central distance

The influence of the central distance (CD) between the elliptical cutout and the auxiliary hole's center on stress concentration was investigated. Figure 10 shows the variation in SCF with the central distance (CD). It is observed that the CD has a slight influence on SCF when the AH diameter is small (d = 6, 12 *mm*), as the obtained data are nearly equal for different CD values. Although increasing AH diameter to d =18 *mm* reduces SCF by 3.5 %, avoiding using a central distance less than (CD = 25 *mm*) is preferable due to the overlapping between the central cutout and auxiliary holes. Also, the area between the closely spaced central cutout and auxiliary holes becomes weak to withstand high applied stress. The CD value is set to 35 *mm* for all tests to find the minimum SCF and maximum RM. The results revealed that the presence of AH can reduce SCF by (1.9 to 25%) and (0.8 to 17 %) for oriented elliptical

cutouts by 45°and 90°, respectively. The results highlight the possible benefits of integrating auxiliary holes into Al-2024 T3 plate to enhance the stress distribution and, consequently, the stress concentration of mechanical parts under tension force. However, finding the optimum orientation angle and auxiliary hole size is not easy.

Table 4. Parameters of Al-2024 T3 plate with oriented elliptical cutout.

Parameter	Base data	Range
d (mm)	6	6-24
ϕ (deg)	0°	0°- 90°

Table 5. The coefficients of the quadratic model.

Coefficient	Z	
	SCF	RM
c_0	1.9092	-0.0075
c_1	0.0534	0.0011
c_2	0.0369	-0.0000
c_3	-0.0003	0.0051
c_4	0.0002	0.0000
c_5	-0.0013	0.0000

5. Surrogated–based optimization

This method obtains the best plate design with cutouts by minimizing the SCF and maximizing the removal mass (RM). The results of the SCF are affected by factors including the size of AH, the space between cutouts, and the orientation angle of the elliptical cutout. The AH diameter and orientation angle significantly influence SCF, while CD has a low effect on SCF. Table 4 lists the processing parameters considered in the experiment's design. The response surface models of SCF and RM are used to evaluate the optimal design solutions. Sixteen design points are considered when generating the response surface model. Polynomial response surfaces of SCF and RM based on d and ϕ are produced by a quadratic model, Eq. 6.

$$Z = c_o + d\ c_1 + \phi\ c_2 + d^2\ c_3 + \phi^2\ c_4 + d\ \phi\ c_5 \tag{6}$$

Where Z, a variable, represents SCF or MR, and c_0 to c_5 represent coefficients. Table 5 lists the quadratic model's coefficients that are fitted for the different response surfaces of stress concentration factor and removal mass, respectively. The response surface models and sample points of stress concentration factor (SCF) and removal mass (RM) are shown in Fig. 11 and Fig. 12, respectively. The created response surfaces optimize SCF and RM based on design variables, including AH diameter (d) and orientation angle (ϕ). These design points are selected based on the sensitivity and significance effect on the objective functions. The response surface models use a quadratic polynomial fitting, which significantly reduces the complexity of computational processing.

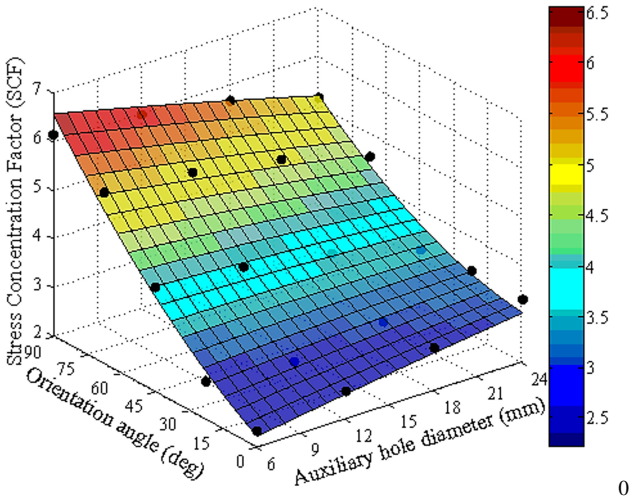

Figure 11. Response surfaces model for SCF in the plate with elliptical cutout and auxiliary hole (AH).

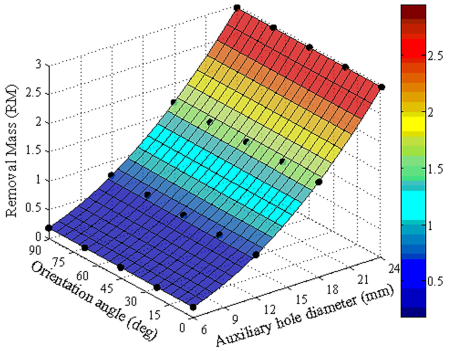

Figure 12. Response surfaces model for RM in the plate with elliptical cutout and auxiliary hole (AH).

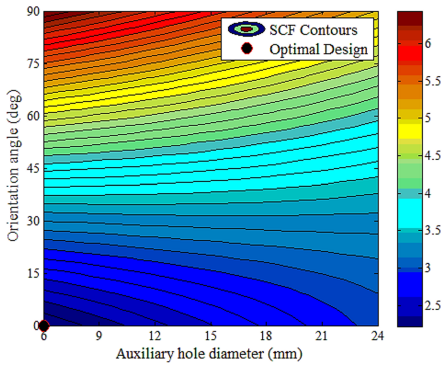

Figure 13. The optimal solution for minimizing SCF in a plate with elliptical cutout and auxiliary holes (AH).

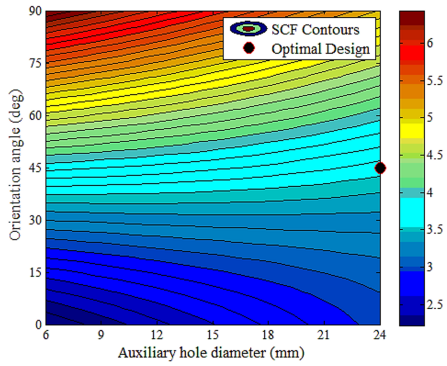

Figure 14. The location of the optimal solution minimizing SCF for the elliptical cutout ($\phi = 45°$) with auxiliary holes (AH).

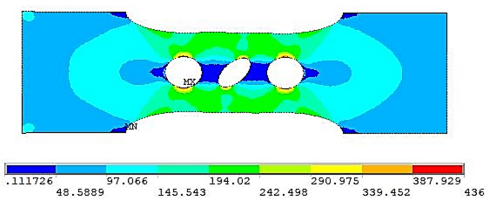

Figure 15. The stress distribution of Al-2024 T3 plate with oriented elliptical cutout $\phi = 45°$and auxiliary holes $d = 24mm$.

5.1 Deterministic optimization

Typically, maintaining reliable strength while reducing SCF and overall plate mass will yield the optimal structure design. Therefore, the function aims to minimize SCF and maximize removal mass (RM) subjected to the constraint of acceptable values of AH diameter (d) and orientation angle (ϕ). The single-objective optimization of SCF and RM is formulated as follows,Eq. 7 and Eq. 8.

$$\begin{aligned} &\underset{d,\ \phi}{\text{Min}} \quad SCF(s) \\ &6 \le d \le 24 \\ &0^\circ \le \phi \le 90^\circ \end{aligned} \tag{7}$$

$$\begin{aligned} &\underset{d,\ \phi}{\text{Max}} \quad RM(s) \\ &6 \le d \le 24 \\ &0^\circ \le \phi \le 90^\circ \end{aligned} \tag{8}$$

SCF (s) and RM (s) are continuous but not necessarily differentiable. The optimal solution indicates that the AH diameter significantly affects the SCF. Figure 13 shows the optimal solution for the plate with an elliptical cutout and auxiliary holes. A black dot marks the location of the optimal solution for minimizing (SCF). This confirms that a minimum SCF occurs when the AH size is small and the orientation angle equals zero.

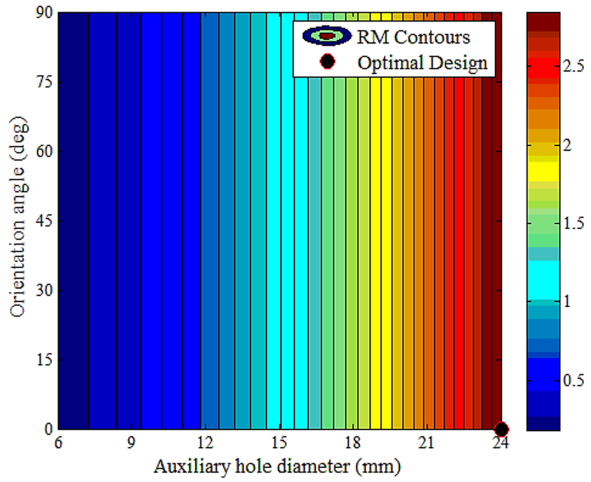

Figure 16**.** The location of the optimal solution for maximizing RMs in Al-2024 T3 plate has an elliptical cutout and auxiliary holes (AH).

Thus, it is recommended that this value be set in the plate design with the cutout aligned horizontally with the loading direction. In contrast, increasing AH diameter leads to minimizing SCF for the plate with an elliptical cutout that is restrained to be greater than or equal to 45 ($\phi \ge 45°$). Figure 14 shows the location of the predicted SCF for the plate with an elliptical cutout oriented by 45°and auxiliary holes. It is found that increasing the AH diameter minimizes SCF significantly and also enhances the stress distribution around the central cutout, as shown in Fig. 15. The maximum stress values are shifted from the oriented elliptical cutout to be on the boundary of AH. Thus, auxiliary holes can decrease the total mass and enhance the stress concentration in Al 2024 T3 plate.Regardless of the elliptical cutout's orientation angle, the removal mass is increased with an increasing AH diameter. Figure 16 shows the location of the maximum RM for the plate with an elliptical cutout and auxiliary holes. However, there is an inverse relationship between objectives. Improving removal mass (RM) requires degradation in the stress concentration factor (SCF). Multi-objective optimization aims to find possible tradeoffs among conflicted multiple objective functions [20]. However, theoretical and computational challenges make solving multi-objective optimization problems difficult. Instead of a single-objective optimization of SCF or RM separately, it would be more accurate to formulate a multi-objective optimization, where the objective functions of SCF and RM are combined as Eq. 9.

$$\begin{aligned} &\underset{d,\ \phi}{\text{Min}} \quad SCF(s) \\ &\underset{d,\ \phi}{\text{Max}} \quad RM(s) \\ &6 \le d \le 24 \\ &0^\circ \le \phi \le 90^\circ \end{aligned} \tag{9}$$

A multi-objective optimization solution is a set of optimums called the Pareto frontier that provides a set of optimal solutions for design variables [30]. Pareto frontier offers more flexibility and optimal solutions than single-objective formulations for decision-makers. The Pareto frontier could be visualized as a curve and surface for two and three objective problems. The optimization problem is solved using a code prepared using the commercial software Matlab [31]. This software incorporates various algorithms and optimizers to be optimally used for the desired design process, which can help make tradeoff decisions to a certain extent. Optimal solutions (Pareto frontier) for Al-2024 T3 plate with different orientation angles of the elliptical cutout and AH diameter are shown in Fig. 17. From Fig. 17, the Pareto frontier reveals that the stress concentration factor is considerably affected by the elliptical cutout orientation angle and auxiliary hole diameter more than the removal mass. Thus, designers can compromise between minimum SCF and maximum RM to select appropriate orientation angles and auxiliary hole diameters based on application requirements.

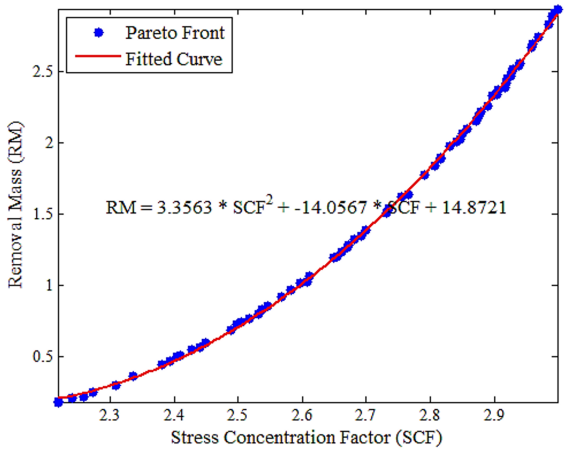

Figure 17**.** Optimal solutions (Pareto frontier) for minimizing SCF and maximizing RM in Al 2024 T3 plate with elliptical cutouts.

6. Conclusions

In this paper, the effect of elliptical cutout orientations on the stress and strain of Al-2024 T3 plates subjected to a tensile load was investigated experimentally and numerically. The numerical model effectively simulates the stress distribution and stress concentration factor (SCF) in Al-2024 T3 plate. The results showed that the value of SCF increases with the order of cutout orientation angle from (ϕ = 0°to 90°). SCF is minimum for the orientation angle (ϕ = 0°), and its value reaches the maximum at the orientation angle (ϕ = 90°). However, adding auxiliary holes can alter the stress distribution and reduce the SCF of Al-2024 T3 plate in the range (1.9 to 25 %). Surrogate-based optimization was used to find the optimal design parameters that affect the stress concentration factor in the plate. Single-objective optimization was formulated to minimize SCF and maximize RM. However, multi-objective optimization is more efficient for finding optimal solutions. Multi-objective optimization is formulated to minimize SCF and maximize RM. For the plate with an elliptical cutout that is restrained to be greater than or equal to 45 ($\phi \ge 45°$), increasing AH diameter leads to minimizing SCF and maximizing RM. Pareto frontier offers reliable, optimal solutions of SCF and RM based on input design parameters. Pareto frontier effectively captured the tradeoff between SCF and RM based on suitable input design variables.

Authors' contribution

All authors contributed equally to the preparation of this article.

Declaration of competing interest

The authors declare no conflicts of interest.

Funding source

This study didn't receive any specific funds.

Data availability

The data that support the findings of this study are available from the corresponding author upon reasonable request.

REFERENCES

[1] A. Barroso and S. Sánchez-Carmona, "Static and fatigue performance of non-circular rivet joints: Comparison between numerical modelling and preliminary testing," *Engineering Failure Analysis*, vol. 162, p. 108364, Aug 2024. [Online]. Available: https://doi.org/10.1016/j.engfailanal.2024108364

[2] S. Rahman, "Stress analysis of finite steel plate with a rectangular hole subjected to uniaxial stress using finite element method," *J. Marine Sci Res Develop.*, vol. 8, no. 3, p. 447–469, 2018. [Online]. Available: doi:https://doi.org/10.4172/2155-9910.1000254

[3] R. H. Patel and B. P. Patel, "Effect of various discontinuities present in a plate on stress concentration: a review," *Eng. Research Express*, vol. 4, no. 3, p. 032001, 2022. [Online]. Available: https://doi.org/10.1088/2631-8695/ac8c1b

[4] T. R. S. C. K S and K. V. Rao, "A parametric study on the effect of elliptical cutouts for buckling behavior of composite plates under non-uniform edge loads," *Lat. Am. j. solids struct*, vol. 17, no. 08, pp. 1–5, 2020. [Online]. Available: https://doi.org/10.1590/1679-78256225

[5] J. R. D. M. Mohammadi and L. Jiang, "Stress concentration around a hole in a radially inhomogeneous plate," *International Journal of Solids and Structures*, vol. 48, no. 3, p. 483–491, 2011. [Online]. Available: https://doi.org/10.1016/j.ijsolstr.2010.10.013

[6] D. Gunwant, "Stress concentration studies in flat plates with rectangular cut-outs using finite element method," *International Journal of Mathematical, Engineering and Management Sciences*, vol. 4, no. 1, p. 66–76, 2019. [Online]. Available: https://dx.doi.org/10.33889/IJMEMS.2019.4.1-006

[7] M. T. Ozkan and I. Toktas, "Determination of the stress concentration factor (kt) in a rectangular plate with a hole under tensile stress using different methods," *Materials Testing*, vol. 58, no. 10, p. 839–847, 2016. [Online]. Available: https://doi.org/10.3139/120.110933

[8] B. Z. W. D. Pilkey, D. F. Pilkey, "Peterson's stress concentration factors, 4th edt. john wiley sons," *General Introductory Mechanical Engineering*, vol. 640, no. 12, p. 8641–8658, 2020. [Online]. Available: https://doi.org/10.1002/9780470211106

[9] S. K. L. Bharambe, "Stress concentration of plate with rectangular cutout," *IRJET*, vol. 06, no. 04, p. 3313–3351, 2019. [Online]. Available: https://www.irjet.net/archives/V6/i4/IRJET-V6I4782.pdf

[10] M. J. J. Rezaeepazhand, "Stress concentration in metallic plates with special shaped cutout," *International Journal of Mechanical Sciences*, vol. 52, no. 1, p. 96–102, 2010. [Online]. Available: https://doi.org/10.1016/j.ijmecsci.2009.10.013

[11] Y. R. M. Kumar and B. Yeshaswini, "Study on the effect of stress concentration on cutout orientation of plates with various cutouts and bluntness," *IJMER*, vol. 3, no. 3, p. 1295–1303, 2013. [Online]. Available: http://www.ijmer.com/papers/Vol3_Issue3/AG3312951303.pdf

[12] M. Patil and A. More, "Effect of hexagonal cutout orientation and roundness of edges on stress concentration in plate," *IRJET*, vol. 08, no. 04, p. 4431–4435, 2021. [Online]. Available: https://www.irjet.net/archives/V8/i4/IRJET-V8I4851.pdf

[13] E. A. M. Jafari, "Stress concentration in finite metallic plates with regular holes," *International Journal of Mechanical Sciences*, vol. 106, no. 3, p. 220–230, 2016. [Online]. Available: https://doi.org/10.1016/j.ijmecsci.2015.12.022

[14] G. Z. Aizhong Lu, Ning Zhang, "Minimizing stress concentrations around an elliptical hole by concentrated forces acting on the uniaxially loaded plate," *Acta Mechanica Solida Sinica*, vol. 30, no. 3, p. 318–326, 2017. [Online]. Available: https://doi.org/10.1016/j.camss.2017.07.002

[15] S. Monti, "Reduction of the local stress field around holes through porous shaped structures," *Communications - Scientific Letters of the University of Zilina*, vol. 20, no. 3, p. 36–41, 2018. [Online]. Available: https://doi.org/10.26552/com.C.2018.3.36-41

[16] B. R. Endigeri and S. G. Sarganachari, "Fem for stress reduction by optimal auxiliary holes in a loaded plate with elliptical hole," *JETIR*, vol. 6, no. 2, p. 517–523, 2019. [Online]. Available: https://www.jetir.org/view?paper=JETIR1902176

[17] D. V. P. Rani and G. Ghangas, "Stress concentration analysis of functionally graded material coated elliptical inclusion under uniaxial tension," *Materials Today: Proceedings*, vol. 78, no. part 3, p. 351–358, 2023. [Online]. Available: https://doi.org/10.1016/j.matpr.2022.09.602

[18] A. Bhosekar and M. Ierapetritou, "Advances in surrogate based modeling, feasibility analysis, and optimization: A review," *Computers Chemical Engineering*, vol. 108, p. 250–267, 2018. [Online]. Available: https://doi.org/10.1016/j.compchemeng.2017.09.017

[19] N. V. S. A. Cozad and D. C. Miller, "Learning surrogate models for simulation-based optimization," *AIChE Journal*, vol. 60, no. 6, p. 2211–2227, 2014. [Online]. Available: https://doi.org/10.1002/aic.14418

[20] O. D. Jumaah, "Experimental and numerical study on manufacturing gallium nitride thin films in mocvd process," *Rutgers University - School of Graduate Studies*, vol. 4, 2019. [Online]. Available: https://doi.org/doi:10.7282/t3-6cxt-ph56

[21] X. Z. S. Gao, Y. Zhao and Y. Zhang, "Application of response surface method based on new strategy in structural reliability analysis," *Structures*, vol. 57, p. 105202, 2023. [Online]. Available: https://doi.org/10.1016/j.istruc.2023.105202

[22] I. Kaymaz and C. McMahon, "A response surface method based on weighted regression for structural reliability analysis," *Probabilistic Engineering Mechanics*, vol. 20, no. 1, p. 11–17, 2005. [Online]. Available: https://doi.org/10.1016/j.probengmech.2004.05.005

[23] H. C. G. P. Ting Lin and Y. Jaluria, "A modified reliability index approach for reliability-based design optimization," *J. Mech. Des.*, vol. 133, no. 4, pp. 1–6, 2011. [Online]. Available: https://doi.org/10.1115/1.4003842

[24] W. W. C. W. S. Obers, J. Overal, "The effect of the yield to tensile strength ratio on stress/strain concentrations around holes in high-strength steels," *Marine Structures*, vol. 84, p. 103205, 2022. [Online]. Available: https://doi.org/10.1016/j.marstruc.2022.103205

[25] E. Madenci and I. Guven, "The finite element method and applications in engineering using ansys®, 2nd ed." *USA: Springer Nature*, p. 2231–2258, 2015. [Online]. Available: https://doi.org/10.1007978-1-4899-7550-8

[26] A. S. W. Young, R. Budynas, "Roark's formulas for stress and strain, 8th edition, 8th edition. new york: Mcgraw hill," *access Engineering*, vol. 18, no. 11, pp. 5394–5409, 2011. [Online]. Available: https://doi.org/10.1109/TWC.2019.2936025

[27] M. V. C. S. J. e. a. A. de A. Neves, Eduardo Coutinho, "Influence of notch geometry and interface on stress concentration and distribution in micro-tensile bond strength specimens," *Journal of Dentistry*, vol. 36, no. 10, p. 808–815, 2008. [Online]. Available: https://doi.org/10.1016/j.jdent.2008.05.018

[28] A. Khaja and R. Rowlands, "Stresses associated with multiple holes whose individual stresses interact ," *The Journal of Strain Analysis for Engineering Design*, vol. 52, no. 3, p. 162–176, 2017. [Online]. Available: https://doi.org/10.1177/0309324717690282

[29] Z. Yang, "The interaction of holes on stress and strain concentrations in uniaxially loaded tensile plates," *Applied Mechanics and Materials*, vol. 268–270, no. 10, p. 767–771, 2012. [Online]. Available: https://doi.org/10.4028/www.scientific.net/AMM.268-270.767

[30] V. P. C. P. S. Parashar, N. Fateh, "Self organizing maps (som) for design selection in multi-objective optimization using modefrontier," *SAE International, Warrendale, PA, SAE Technical Paper*, vol. 2008, no. 5, p. 01–0874, 2008. [Online]. Available: [Online].Available:https://doi.org/10.4271/2008-01-0874

[31] A. Messac, "Optimization in practice with matlab®: For engineering students and professionals," *1st ed. New York, USA: Cambridge University Press, 2105*, vol. 26, no. 5, p. 1150–1154, 2022. [Online]. Available: www.cambridge.org/9781107109186

How to cite this article:
Rwaa Talal Abdullah, Omar D. Jumaah, and Yogesh Jaluria. (2025). 'Surrogated based optimization of stress concentration in Al-2024 T3 plate with elliptical cutout under uniaxial loading', Al-Qadisiyah Journal for Engineering Sciences, 18(2), pp. 148-154. https://doi.org/10.30772/qjes.2024.153041.1371